**COMMUNICATIONS IN SCIENCE AND TECHNOLOGY**
*Homepage:* cst.kipmi.or.id

# Adsorption studies of KOH-modified hydrochar derived from sugarcane bagasse for dye removal: Kinetic, isotherm, and thermodynamic study

Dwi Indah Lestari, Ahmad Tawfiequrrahman Yuliansyah*, Arief Budiman

*Department of Chemical Engineering, Universitas Gadjah Mada, Yogyakarta 55281, Indonesia*

*Article history:*
Received: 5 January 2022 / Received in revised form: 25 May 2022 / Accepted: 30 May 2022

**Abstract**

Toxicity of methylene blue (MB) in water bodies has a negative effect on environment and living organisms. The presence of MB in water could last longer in view of the non-biodegradable characteristic. In this study, hydrochar was used as adsorbent to remove MB from aqueous solution. Hydrochar derived from bagasse was successfully prepared by hydrothermal carbonization treatment at temperature of 270ºC, and pressure of 10 Bar for 30 minutes. For enhancing the adsorption ability, hydrochar was activated by adding KOH that was able to increase the percent removal by ~11%. The hydrochar was characterized using FTIR before and after adsorption. The results showed that the dominant functional groups of hydrochar included O-H, C=O, -O- and aromatic compounds. Whereas, the functional group of azo groups such as N-H and N=N appeared after adsorption. The maximum adsorption capacity ($Q_{max}$) was 5.1204 mg/g, while the adsorption isotherm of MB onto hydrochar followed the Langmuir and Freundlich model. The adsorption mechanism belongs to chemical adsorption, and the rate of diffusion can be neglected because the adsorption kinetics fitted well with pseudo-second order and the value of $k_2 > k_{dif} > k_1$. Thermodynamic studies indicated that the adsorption process is classified as endothermic and reversible at room temperature. The results showed that hydrochar could be the alternative adsorbent for removing MB in wastewater. In addition, sugarcane bagasse has a great potential as feedstock of hydrochar.

*Keywords:* Hydrochar, Hydrothermal Carbonization; Adsorption; Methylene blue; Sugarcane Bagasse

## 1. Introduction

Industry plays an important role in country's economic development. Rapid industrialization has been driven by the high demand for goods. Nowadays, the world is entering Industry 4.0 towards the manufacturing industries, one of which was textile industry. As the population increases, one of the primary needs such as garments or apparel will always increase.

The practice of industry 4.0 aims to build the efficient industrial components related to the production process management system independently[1]. Industry 4.0 has a mission to increase productivity up to 55% and profits by 16%[2]. In Indonesia, this implementation is known as "Making Industry 4.0". As revealed by the report in 2015-2019 from the Ministry of Industry, Indonesia has exported the textile and garment for about USD 8, 83 million.

In the perspective of economy, this is a good chance to enhance the export values. In contrast to the perspective of environment, it is a challenge for engineers to control the potential pollution. Textile industry wastewater is mostly found in dyeing, printing, and finishing process due to the high demand for water consumption. About 10-15 % of the dye is wasted along with the wastewater during the process. These dyes and its chemicals are undesirable in the environment because of their toxic nature after degradation, and it can contaminate the soil, sediment and surface water[3].

Some dyes have carcinogenic, toxic and mutagenic impact. Furthermore, dyes that contaminate water bodies could interfere with aquatic plant biological activity, reducing sunlight penetration due to the formation of a thin layer between the water surface and air[4].

Each dye has its own chemical structure that has a certain effect if it accumulates in excess. Of dyes, Methylene Blue (MB) is widely used for dyeing clothes and paper, redox indicator and nucleic acid detector [5]. It has the chemical formula of $C_{16}H_{18}N_3ClS$. About 5 % of the total MB used in dyeing process can be utilized, the residual will be released with wastewater[6]. Even at extremely low concentrations, the presence of MB in water bodies can produce brightly colored byproducts. It diminishes oxygen solubility, impairs the photosynthetic activity of aquatic life, and limits the diversity and appearance of the biological community due to its high molar absorption coefficient, which reduces sunlight transmission. MB presence in water bodies, even at a very low concentration, makes highly colored sub-products [7]. Long-term exposure of MB can cause methemoglobinemia, nausea, anemia and hypertension [8], even exposure of ≥ 18 mg/L can interfere with aquatic life [9]

Several methods including flocculation, coagulation, chemical precipitation, advanced oxidation, reverse osmosis, and adsorption have been applied to reduce the contaminant. In this case, adsorption has received so much attention due to its

* Corresponding author.
Email: atawfieq@ugm.ac.id
https://doi.org/10.21924/cst.7.1.2022.669

simple method and effective in removing contaminants in wastewater [10]. The adsorbent that is generally used is activated carbon, but several studies have shown that the solid product from HTC, hydrochar, has the potential for adsorbent use.

Hydrothermal is a thermal degradation process converting biomass without pre-treatment of drying [11]. The HTC process requires a lower temperature of 180-350ºC, pressure of 10-80 Bar [12]and a holding time of 5-240 minutes. Generally, in the HTC process, water is used as a solvent or medium that contributes to hydrolysis process [13]. The HTC process consists of several stages such as hydrolysis, dehydration and fragmentation, polymerization and aromatization, the growth of hydrochar particles [14].

Previous study of hydrochar adsorbent was carried out by several researchers including bamboo hydrochar modified with NaOH using cold alkali activation [15], pine wood hydrochar with oxidation treatment[16], utilization of sewage sludge and coconut shell as hydrochar with KOH modification[17], and coffee-husk hydrochar prepared by hydrothermal and soaking methods[18]. These studies showed that the addition of an activating agent could increase certain functional group on hydrochar.

This experiment utilized sugarcane bagasse as a feedstock for making hydrochar. It was selected as the sugar milling process in the sugar factory generally produces the abundance of bagasse as by-product. Moreover, Indonesia has 415,663 Ha of sugarcane plantation area, mostly used for sugar factories [19]. Hence, the utilization of this biomass could answer the two problems at once, first the textile industry wastewater, and second the sugar factory by-product.

The novelty of this experiment is the use of hydrochar derived from sugarcane bagasse to adsorb the methylene blue from aqueous solution. The ability of the hydrochar was evaluated by kinetic, isotherm, and thermodynamic studies representing the adsorption criteria occurred during process. The hydrochar characteristics was also analyzed using Fourier Transformed Infrared (FTIR) Spectroscopy.

## 2. Materials and Methods

This research consists of four stages started from the preparation of raw materials, hydrochar synthesizing, hydrochar modification and adsorption studies with the reference of the previous research [20].

### *2.1. Preparation of Sugarcane Bagasse*

Sugarcane bagasse was obtained from Madukismo Sugar Factory in Special Region of Yogyakarta. Sugarcane bagasse was cut into small pieces and milled into grinder. The fine bagasse was then sieved with Tyler screen with the particle size of -32 +48 mesh.

### 2.2. *Hydrothermal Carbonization* (HTC)

The HTC process for sugarcane bagasse was conducted in a closed stainless-steel autoclave (figure 1). 15 g of bagasse was added with 150 mL distilled water. The mixture was then placed inside the autoclave.

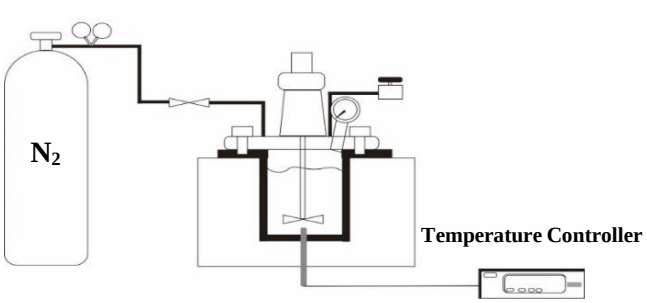


Fig. 1. Schematic diagram of Hydrothermal Carbonization

Before the process started, the autoclave was purged by draining off the $N_2$ gas into autoclave, and then drained out the using purge valve (purging with 3 repetitions). Once purging was finished, the pressure was adjusted to 10 bar gauge and the heater was turned on and adjusted to the set point. The process temperature was adjusted into 270ºC with 30 minutes of holding time. The temperature was chosen because our previous study has shown that the hydrochar produced from this temperature could result in the highest removal percentages. During the process, the stirrer was turned on to make the heat distribution equal. Once completing the process and cooling the autoclave down for a while, the product in the form of slurry was obtained. The product was then separated using vacuum filtration. The solid product (hydrochar) was heated for 4 hours at 105ºC and the product was labeled as SHC270.

### *2.3. KOH modification of Hydrochar*

2 g of the obtained hydrochar was mixed with 0.5 N KOH 200mL at room temperature for 1 hour. Afterwards, the mixture was filtered using vacuum filtration to obtain the modified hydrochar. In addition, the modified hydrochar was dried in an oven at 105ºC for 4 hours. The modified hydrochar was then labeled as ACSHC270.

### *2.4. Characterization*

The functional groups of sugarcane bagasse and hydrochar before and after adsorption were analyzed using Fourier Transform Infrared (FTIR) Spectroscopy at a wavelength of 400 – 4000 $cm^{-1}$. Furthermore, to investigate the evolution of the structure and the functional groups of hydrochar occurred during the carbonization process, the FTIR Spectroscopy analysis was performed to hydrochars produced from different temperatures (200, 240, and 300ºC). These hydrochars were called as SHC200, SHC240, and SHC300 respectively.

### *2.5. Adsorption Studies*

The adsorption isotherm was carried out by preparing the MB solution with initial concentration range of 20-60 mg/L. The solution was then added with 0.5 g of hydrochar. Each erlenmeyer was placed in a shaker water bath for 120 minutes at 30ºC. The solution was then filtered with 0.22µm syringe filter. Meanwhile, the MB concentrations were measured using UV-Vis Shimadzu Mini 1240 at 663 nm. Equilibrium concentration of MB ($C_e$) was determined using the equation from calibration curve. The amount of MB adsorbed in

adsorbent was calculated using eq. (1) and the percentage removal of MB (%R) was calculated using eq. (2).

$$Q_e = \frac{(C_o - C_e)V}{W} \quad (1)$$

$$\% R = \frac{C_o - C_e}{Co} x100 \quad (2)$$

$C_o$ (mg/L) and $C_e$ respectively represent the initial concentration and the equilibrium concentration of MB. V (L) is the volume of adsorbate and W (g) is the mass of adsorbent.

Langmuir and Freundlich isotherm are two isotherm models widely used to describe the adsorption phenomenon. Langmuir isotherms assumes that adsorption is a monolayer where the amount of adsorbate will attach a finite number of adsorption sites[21]. The Langmuir isotherm is expressed in the following equation (3)

$$Q_e = \frac{Q_{max}.C_e.K}{1+K.C_e} \quad (3)$$

Equation (3) is liniearized by plotting y-axis ($C_e/Q_e$) and x-axis ($C_e$), so that equation (3) becomes eq. (4)

$$\frac{C_e}{Q_e} = \frac{C_e}{Q_{max}} + \frac{1}{Q_{max}.K_L} \quad (4)$$

where $Q_{max}$ is the maximum adsorption capacity (mg/g), $Q_e$ is the adsorption capacity at equilibrium, and $K_L$ (g/L) refers to the Langmuir constant.

Meanwhile, Freundlich isotherm depicts that the adsorbate attach into heterogeneous surfaces where the distribution of active sites is not uniform and adsorption occurs in a multilayer manner. Freundlich isotherm represented in equation (5).

$$Q_e = K_F.C_e^{\left(\frac{1}{n}\right)} \quad (5)$$

Equation (5) was linearized by adding the logarithm on left and right sides, so that the eq. (6) was obtained.

$$\ln Q_e = lnK_F + \frac{1}{n}.lnC_e \quad (6)$$

$C_e$ defines the concentration of adsorbate in equilibrium (mg/L), $Q_e$ indicates the miligram of adsorbate attached in grams of adsorbent or adsorption capacity at equilibrium (mg/g), and Freundlich constanta is $K_F$ (mg/g)(L/mg)$^{1/n}$. Further, 1/n indicated the Freundlich isotherm equilibrium constant as a degree of non-linearity between solution and solute.

The kinetic adsorption consists of 3 steps, i.e. external diffusion, internal diffusion and adsorption. The kinetic model aims to investigate the adsorption mechanisms that occurs between adsorbate and adsorbent started from the initial step into equilibrium step. The kinetic models used in this experiment were pseudo first order and pseudo second order.

The pseudo first order (PFO) model was empirically by Lagergen in 1898[22]. The PFO model expressed in eq. (7)

$$\frac{dQ_t}{dt} = k_1(Q_e - Q_t) \quad (7)$$

The equation was linearized by integrating eq.(7) at the boundary conditions of t=0 and $Q_t$ = t to t = t and $Q_t = Q_t$, so that the equation resulted in eq. (8) or (9)

$$\log(Q_e - Q_t) = \log Q_e - \frac{k_1}{2.303}.t \quad (8)$$

or,

$$\ln(Q_e - Q_t) = \ln Q_e - k_1.t \quad (9)$$

$k_1$ (min$^{-1}$) refers to the PFO rate constant, and $Q_e$ and $Q_t$ (mg/g) is adsorption capacity at equilibrium and at the time-t.

Thereafter, the pseudo second-order (PSO) kinetic was empirically applied by Ho in 1996 [23]. The equation was expressed in equation (10).

$$\frac{dq_t}{dt} = k_2(Q_e - Q_t)^2 \quad (10)$$

By integrating the equation (10) at the boundary conditions t=0 and $Q_t$ = t to t = t and $Q_t = Q_t$ so that the equation (10) becomes eq. (11).

$$\frac{t}{Q_t} = \frac{1}{k_2.Qe^2} + \frac{t}{Qe} \quad (11)$$

$k_2$ (g.mg/min) refers to the PFO rate constant, and $Q_e$ and $Q_t$ (mg/g) is adsorption capacity at equilibrium and at the time-t.

Commonly, the pseudo-first order kinetic is encountered in the adsorption with a very high $C_o$ value, and this model, which is frequently recognized during the early stages of adsorption, has a limited number of active sites. Meanwhile, pseudo-second order kinetic often encountered in the adsorption with a lower $C_o$, and commonly observed at the final stage of adsorption, contains the abundance of active sites on it [24]. Furthermore, to observe more about the rate-controlling step mechanism on this adsorption, the Weber-Morris model, namely intra-particle diffusion was described about the mechanisms or movement of adsorbate molecules from liquid to solid phases (adsorbent) [17]. This model can be seen in equation (12).

$$Q_t = k_{dif}\ t^{0.5} + C \quad (12)$$

where $Q_t$ refers to adsorption capacity at the time-t, $k_{diff}$ indicates rate constant intra-particle diffusion, and the intercept is depicted with C associated with boundary layer thickness.

Furthermore, the study on the adsorption behavior that occurs in the adsorption of MB onto hydrochar was explained through thermodynamic adsorption. The thermodynamic parameter aimed to assign if the process was reversible or irreversible, exothermic or endothermic. The thermodynamic parameters can be obtained by following equation (13).

$$\Delta G^o = -RT \ln K_c \quad (13)$$

$$K_c = \frac{Q_e}{C_e} x \frac{W}{V} \quad (14)$$

Furthermore, van't hoff equation was used to observe the value of $\Delta H^o$ and $\Delta S^o$ using equation (eq. 15).

$$lnK_c = \frac{\Delta S^o}{R} - \frac{\Delta H^o}{RT} \quad (15)$$

where R represents the gas constant 8.314 J/mol.K, $K_c$ represents equilibrium constant, and T (K) refers to temperature.

The thermodynamic criteria were based on the values of $\Delta G^o$, $\Delta H^o$ and $\Delta S^o$ obtained. If the value of $\Delta G^o$ was negative, the process was spontaneous (irreversible). While, the positive value indicated reversible adsorption. Moreover, a positive value of $\Delta H^o$ denoted an endothermic reaction, whereas a negative value indicated an exothermic process. While the value of $\Delta S^o$ depicts the affinity between the adsorbent and the adsorbate.

Furthermore, the additional derivative from Langmuir Isotherm model was the separation factor ($R_L$)used to

determine the adsorption tendency. The equation is expressed in eq. (16)

$$R_L = \frac{1}{1+K_L C_o} \quad (16)$$

The $R_L$ value describes the adsorption conditions between the adsorbate and the adsorbent. The value $R_L = 0$ indicates the reversibility of adsorption, while $R_L > 0$ denotes that the adsorption in unfavorable. The range value of $0 < R_L < 1$ refers to favorable adsorption.

## 3. Results and Discussion

### *3.1. FTIR Analysis*

The changes of functional group in hydrochar were observed using FTIR (figure 2). The FTIR result showed that both samples had a similar peak. The strong peak at ~ 3345.19 - 3418.46 $cm^{-1}$ showed the existence of O-H group derived from hemicellulose, cellulose and lignin [25]. The decrease in intensity of O-H group was determined by several factors, such as hemicellulose, which started to hydrolize at 200ºC followed by dehydration of cellulose during heating. Cellulose started to degrade at 210ºC and completely decomposed at 260ºC [26].

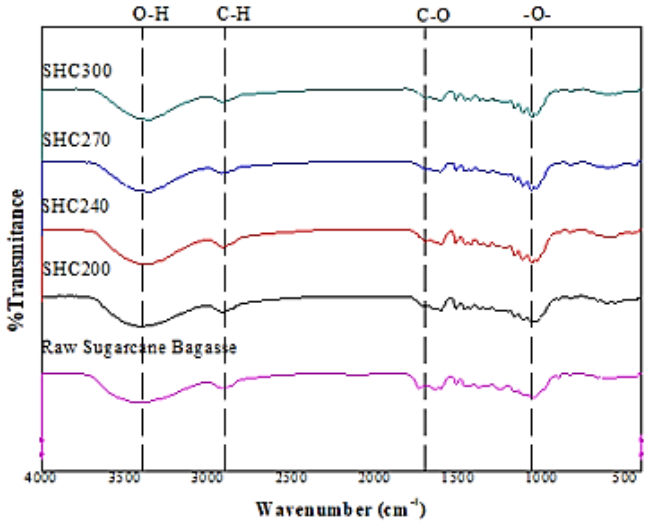


Fig 2. FTIR analysis of Raw Sugarcane Bagasse and Hydrochar at Various Temperatures (200 – 300ºC)

Both sugarcane bagasse and hydrochar showed the peaks in the range of ~2905.50 – 2918.05 $cm^{-1}$ indicating the aliphatic structure inside. This group withstood from 200 to 300ºC, and the saturated aliphatic characteristics were difficult to react. Furthermore, the small peak found in SHC200 showed the presence of a methoxy group with lower intensity ($C-H_3$) indicating a transformation of phenolic compounds during heating, but this functional group was degraded at temperature >200ºC. The peak at 1696.04 – 1734.20 $cm^{-1}$ referred to ketone group (C=O) derived from cellulose and hemicellulose structure in which the increase in the intensity of C=O at the range temperature of 200 – 270ºC was related to the formation of glucose derived from cellulose. The glucose then reacted through the tau-tomerism reaction, aldol condensation and dehydration to form an aldehyde group, and a soluble product in the form of furfural[27].

The weak peak C≡C found on sugarcane bagasse in peak of 2128.22 $cm^{-1}$ indicated the transition of carbonyl groups or monosubstituted alkynes. Hereinafter, the strong peaks in the range of ~1631.32 – 1635.08 $cm^{-1}$ were found in sugarcane bagasse samples and SHC200 and disappeared with the increasing temperature >200ºC. Mostly, amide group are soluble in water so that the elevating temperature above 200ºC could release amide groups, which are initially bound to sugarcane bagasse and dissolved into the water.

The peak range of ~1605.23 – 1608.77 $cm^{-1}$ and 1513.57 – 1514.10 $cm^{-1}$, which were found in all samples indicated the stretching of the aromatic compounds. This aromatic structure was derived from the lignin component[28]. The increase in the intensity of aromatic structure from a temperature of 200 to 300ºC was in view of the main mechanisms step of HTC, i.e. aromatization.

Ester functional group (-COO-) was found in sugarcane bagasse and SHC200 at 1235.26 – 1249.69 $cm^{-1}$ [29]. This group was formed due to the breakdown of cellulose chain during hydrolysis reaction [30]. At the temperature > 200ºC, esters have already been into several compounds such as organic acid and decarboxylated. The peak at 1032.96 – 1033.84 $cm^{-1}$ were found in all samples derived from the lignin structure. The decomposition was indicated by the intensity of ether group (-O-) starting to decrease from the temperature of 200 – 300ºC

Furthermore, FTIR characterization was carried out on samples before and after adsorption of MB to discover the functional groups that played a role in MB adsorption. By knowing the functional groups formed, it can be assumed the several mechanisms existed between the adsorbent and the adsorbate. Figure 3 shows the results of the FTIR analysis.

The new functional group appeared at 2341 and 2077 $cm^{-1}$ after MB adsorption (figure 3) as indicated with the N-H and N=N components of the azo group [31]. Meanwhile, the mechanisms that occurred included (1) H-Bonding on char and N molecules in methylene blue, (2) electrostatic attraction between O atoms and N atoms from N=N group in methylene blue, or (3) π- π interaction between the aromatic groups on char and methylene blue.

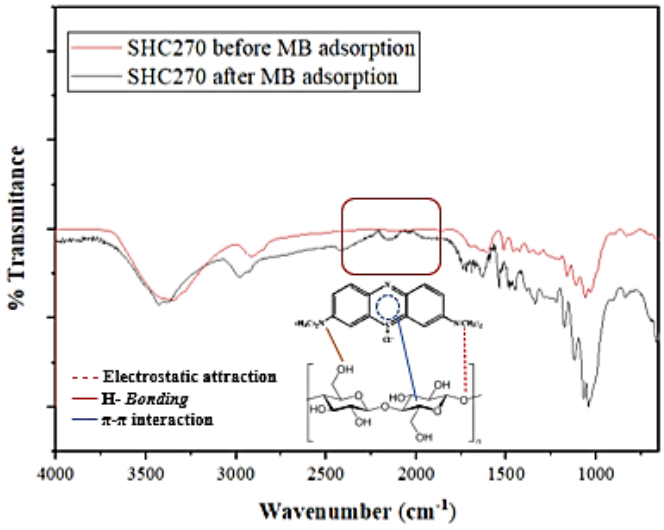


Fig 3. The Comparison of FTIR analysis between Hydrochar Adsorbent (SHC270) before and after Methylene Blue Adsorption

### 3.2. Isotherm Study

The adsorption isotherm describes the distribution of adsorbate (MB) in the solid (adsorbent) and liquid phases at equilibrium circumstances and constant temperature. Hence, the initial concentration is varied to determine the isotherms adsorption behavior and the performance of hydrochar in adsorbing cationic dyes in low and high concentrations. Table 1 shows the ability of hydrochar to adsorb MB at higher and lower concentrations.

Table 1. Initial concentration ($C_o$) variation of MB by SHC270

| Initial Concentration, $C_o$ (mg $L^{-1}$) | $C_e$ (mg $L^{-1}$) | $Q_e$ (mg $g^{-1}$) | %R | $R_L$ |
|---|---|---|---|---|
| 20 | 0.119 | 1.973 | 99.40 | 0.027 |
| 30 | 0.632 | 2.912 | 97.89 | 0.018 |
| 40 | 2.508 | 3.737 | 93.73 | 0.014 |
| 50 | 5.773 | 4.392 | 88.45 | 0.011 |
| 60 | 9.585 | 5.001 | 84.03 | 0.009 |

The removal at the initial concentration of 20 mg/L was 99.40 percent, whereas the percentage of removal at the maximum MB concentration of 60 mg/L was 84.03 percent. The researchers concluded that adsorption was significantly higher at lower adsorbate concentrations. At the higher concentration of adsorbate, the active site on the adsorbent will become easily saturated because the available active site is limited but the MB molecules are higher[32]. This phenomenon shows that some MB molecules have covered all of the active sites; while, other MB molecules that have not been adsorbed will accumulate around the adsorbent surface, making the mass transfer between MB molecules and sorbent surface slower. It indicates that the process has a lower removal percentage at the higher concentration of MB [33]. This occurs due to the fewer number of active sites on the adsorbent, so that only several molecules of MB could attach to the active site.

Figure 1 illustrates the fitting isotherm curve and figure 2 showed that the adsorption tended to follow the isotherm models because the fitting curves on both isotherm models provided a regression value ($R^2$) above 0.9. Generally, the process occurred because the active site of the adsorbent was less than the adsorbate molecule. The adsorption started with the monolayer formation, after the first layer was fulfilled and then the second layer was formed into a multilayer. This model has the characteristic of monolayer adsorption and classified into chemisorption process[34].

Another parameter obtained from isotherm study was $R_L$. This constant described the separation factor derived from Langmuir model. In this adsorption, the $R_L$ value was in the range of 0.0092 – 0.0271, which was included in the range of $0<R_L<1$, indicating that the adsorption was favorable and the process was more suitable in the lower concentration [35]. The *n* value in freundlich isotherm intended to exhibit physical process on it. The n value more than 1 (n>1) indicated that the adsorbate molecule was trapped on the different size of pore surface in the adsorbent [36].

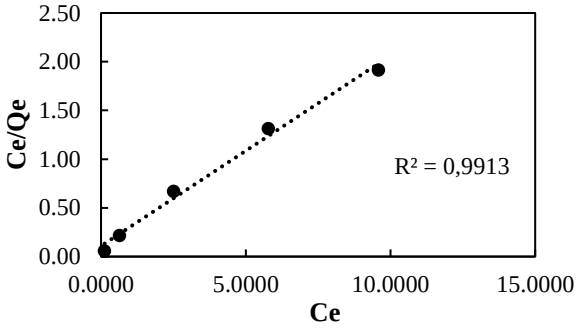


(a)

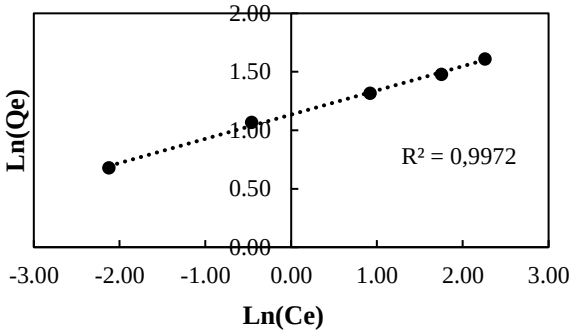


(b)

Fig. 4. Plotting result of adsorption isotherm of MB adsorption onto Hydrochar (a) Langmuir, (b) Freundlich Isotherm

Table 2. The Isotherms Parameter and its Coefficients

| Parameter | Langmuir Isotherm | Parameter | Freundlich Isotherm |
|---|---|---|---|
| $Q_{max}$ (mg $g^{-1}$) | 5.120 | n | 4.831 |
| $K_L$ (L $mg^{-1}$) | 1.797 | $K_f$ (mg $g^{-1}$)(L $mg^{-1})^{1/n}$ | 3.108 |
| $R^2$ | 0.991 | $R^2$ | 0.997 |
| SSE | 1.286 | SSE | 0.047 |

### 3.3. Kinetic Study

The kinetic adsorption intends to investigate the rate of adsorption and how long the hydrochar adsorbent could adsorb the adsorbate until reaching equilibrium. Figure 5 shows the relationship between the adsorption capacities and the adsorption time with various initial concentrations of MB.

As shown in figure 5, the MB adsorption for all initial concentration (IC) variations (20-50 mg/L) has already reached equilibrium in 20 minutes. The adsorption with IC of 30 mg/L and 40 mg/L had decreased the adsorption capacity at t=10 minutes, but after 20 minutes the adsorption capacity began to increase and showed a stable curve. In the initial step of adsorption, the active sites were not fully bound so that some molecules were released or desorbed. The study conducted by Hao-Zhe Li (2021) showed that the rate of adsorption increased faster at the first 120 minutes and become slower until approaching the equilibrium phase in 360 minutes [37].

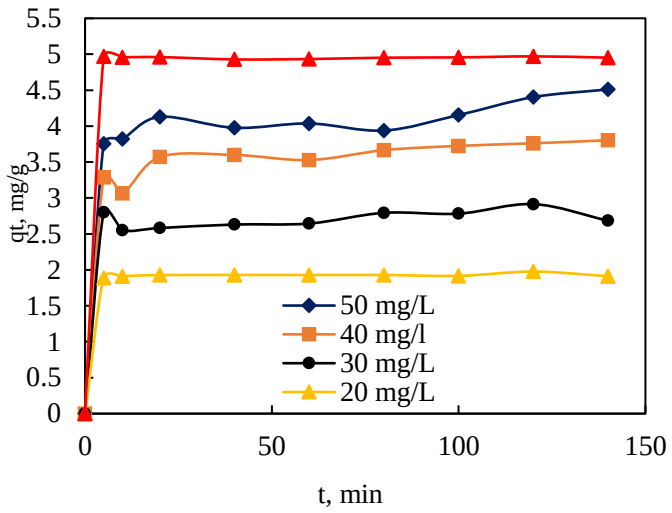


Fig. 5 Kinetic study on various initial concentration of MB

This phenomenon was related to the results of the isotherm model, which stated that MB adsorption onto hydrochar followed both Langmuir and Freudlich isotherms. This explains the phenomenon during the initial adsorption, when all of the active sites were fulfilled with adsorbate molecules, some of MB molecules that have not been bound would form a new layer and begin to form a multilayer pattern as the characteristic of Freundlich isotherm. It should be noted that molecules with a high affinity will be bounded strongly into the active site of adsorbate. As a result, the more the layers are formed, the weaker the affinity between the adsorbate and the adsorbent. Then, the bounding will be easily separated.

The comparison between the adsorbent SHC270 and ACSHC270 showed that the activated adsorbent had a higher and more stable adsorption ability. The adsorption capacity for ACSHC was 4.9 mg/g higher than SHC270 with 3.7 – 4.5 mg/g adsorption capacities. This indicated that ACSHC270 has a better decolorant or contaminant removal ability.

Table 3. Kinetic parameters of pseudo 1st order and pseudo 2nd order

| Initial Concentration of MB, $C_o$ (mg $L^{-1}$) | Adsorbent Type | Pseudo 1st Order Parameter | | Pseudo 2nd Order Parameter | |
|---|---|---|---|---|---|
| | | $k_1$ ($min^{-1}$) | $R^2$ | $k_2$ (g/(mg.min)) | $R^2$ |
| 20 | SHC270 | 0.017 | 0.244 | 2.269 | 1 |
| 30 | SHC270 | 0.016 | 0.309 | 0.974 | 0.974 |
| 40 | SHC270 | 0.026 | 0.668 | 0.607 | 0.999 |
| 50 | SHC270 | 0.014 | 0.383 | 0.503 | 0.998 |
| 50 | ACSHC270 | 0.034 | 0.305 | 0.342 | 1 |

The adsorption kinetic parameter results were tabulated in table 3 using pseudo first order and pseudo second order equations. The results denoted that the adsorption was fitted well with pseudo second order because it gave a regression ($R^2$) value of ~0.9, while the pseudo first order gave an average regrresion range ($R^2$) of ~0.3. This indicated that the rate controlling step was a chemical reaction and the interaction occurred in adsoprtion was dominated by chemical interaction[17]. The interaction that occurred during adsorption was chemical interaction between the polar functional groups and MB molecules on the hydrichar surface[23]. The previous study explained that the MB adsorption was fast (reaching the equilibrium stage after 60 minutes) and the kinetic model followed the pseudo second order [38].

Table 4. Intra-particle diffusion parameter mechanisms

| Initial Concentration (mg $L^{-1}$) | Adsorbent Type | Parameter | |
|---|---|---|---|
| | | $k_{dif}$ (g/(mg.min))$^{0.5}$ | $R^2$ |
| 20 | SHC270 | 0.090 | 0.388 |
| 30 | SHC270 | 0.135 | 0.388 |
| 40 | SHC270 | 0.203 | 0.499 |
| 50 | SHC270 | 0.227 | 0.476 |
| 50 | ACSHC270 | 0.226 | 0.332 |

The Weber-Morris model, specifically intra-particle diffusion, was utilized to explore the rate limiting stage in the adsorption process. The parameter result was tabulated in table 4. The parameter in the form of regression ($R^2$) and k values were compared between the pseudo second ordermodel and the intra-particle diffusion model. The resuts showed that the regression value ($R^2$) of pseudo second order model was greater than intra-particle diffusion. in addition, the value of $k_2$ was smalller than $k_{diff}$ that indicated that the diffusion was not the rate limiting step in this adsorption.

As shown in table 4, it can be obseved that as the initial concentration of MB increasing, the value of rate of diffusion, $k_{diff}$, increased and this indicated the increasing reaction force that facilitated the diffusion.

The thickness impact of the boundary layer on the adsorbent is described by the C coefficient in the Weber-Morris Equation. The greater the C-value, the thicker the boundary layer; hence, the rate of diffusion could not be neglected[39]. The adsorbate will be moved slowly through the boundary layers into the active sites of adsorbent if the adsorption is controlled by diffusion [40].

However, this experiment showed that the adsorption did not fitted well with Weber-Morris model, and the rate of diffusion could be neglected due to the assumption of the thin boundary layer and the small particle of hydrochar.

### *3.4. Thermodynamic Study*

Thermodynamic study of methylene blue using hydrochar was carried out at various temperatures of 303K, 313 K, and 323 K for 120 minutes. This study aims to determine whether an adsorption is more suitable at room temperature or requires further heating. Figure 6 shows the high correlation between in

$K_c$ and 1.T meaning that the temperature affects the adsorption rate.

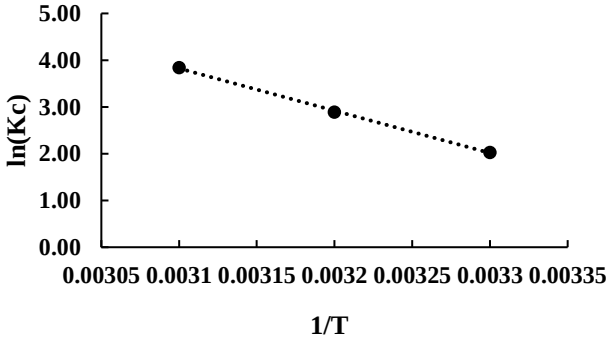


Fig. 6. Van't Hoff plotting in thermodynamic study

The thermodynamic parameters obtained from Van't Hoff plotting between ln $K_c$ and 1/T are tabulated in Table 5. The parameters obtained included enthalpy ($\Delta H^o$), Gibbs Free Energy ($\Delta G^o$) and entropy ($\Delta S^o$). Thermodynamic study intended to predict or assume whether the adsorption was chemisorption or physisorption, irreversible or reversible, and endothermic or exothermic[41].

Table 5. Thermodynamic results on MB adsorption using SHC270

| Temperature (K) | Ce (mg/L) | $Q_e$ (mg/g) | Kc | $\Delta G^o$ (kJ/mol) | $\Delta H^o$ (kJ/mol) | $\Delta S^o$ (kJ/mol) |
|---|---|---|---|---|---|---|
| 303 | 5.773 | 4,392 | 7,607 | -5,069 | | |
| 313 | 2.614 | 4,711 | 18,026 | -7,719 | 75,208 | 0,2469 |
| 323 | 1.047 | 4,863 | 46,446 | -10,368 | | |

The negative values of Gibbs free energy ($\Delta G^o$) at all adsorption temperatures (303, 313 and 323 K) indicated the spontaneously reaction[42]. As the increasing temperature, the mobility of MB molecules also increased; hence, the affinity of adsorbate and adsorbent's active site was getting stronger. The adsorption process was endothermic and favorable at higher temperature according to the value of $\Delta H^o$ and $\Delta G^o$.

At an adsorption temperature of 323 K, the adsorbent structure was more open and the adsorbate was more easily attached to the active site of adsorbent. The increasing temperature has made the viscosity of the liquid decreased and the rate of diffusion in adsorbate through boundary layer and internal pore of the adsorbent increased [43]. This tendency occurred when the saturation value was attained, and the adsorption was considered to be promoted by high temperature and occupied an inactive site onto adsorbents [44]

The enthalpy parameter ($\Delta H^o$) predicted the adsorption mechanisms such as chemisorption or physisorption. The result showed that the enthalpy value of 75.2084 kJ/mol included in the range of $20.9 < H^o < 418.4$ kJ/mol, showing that the adsorption is included in chemical adsorption [42].

## 4. Conclusion

The experimental results showed that the hydrochar adsorbent made from sugarcane bagasse provided an alternative solution to utilize agriculture waste and reduce dye contaminant from textile industry. Hydrochar could adsorb the methylene blue with a percentage of removal ranging from 84 to 99 %. The FTIR result showed that the hydrochar was dominated by O-H, C=C groups and aromatic compounds on it. Modified KOH increased the percentage of removal ~11% and increased the adsorption capacity from 4.3919 mg/g to 4.9750 mg/g. adsorption isotherm study indicated that adsorption followed both Langmuir and Freundlich isotherm. Meanwhile, the adsorption kinetics following the pseudo second order with a rate controlling step was chemical reaction. The thermodynamic studies showed that the adsorption temperature of 323 K can be used as a recommendation for further experiment because at that temperature, the adsorption capacity increases and the adsorption is irreversible.

## Acknowledgements

Author would like to acknowledge the financial support from the Faculty of Engineering, Universitas Gadjah Mada.

## References

1. Gunawan *et al. Transformasi Industri 4.0 Manufaktur Proses Tekstil dan Apparel*. (Pusat Pengembangan Pendidikan Vokasi Industri Badang Pengembangan Sumber Daya Manusia Industri Kementrian Perindustrian Republik Indonesia, 2021).
2. Majumdar, A., Garg, H. & Jain, R. *Managing the barriers of Industry 4.0 adoption and implementation in textile and clothing industry: Interpretive structural model and triple helix framework*. *Comput. Ind.* 125 (2021) 103372.
3. Yaseen, D. A. & Scholz, M. *Textile dye wastewater characteristics and constituents of synthetic effluents: a critical review*. *International Journal of Environmental Science and Technology* vol. 16 (Springer Berlin Heidelberg, 2019).
4. Mani, S. & Bharagava, R. N. *3 Textile Industry Wastewater Environmental and Health Hazards and Treatment Approaches*. II (2018).
5. Shakoor, S. & Nasar, A. *Utilization of Punica granatum peel as an eco-friendly biosorbent for the removal of methylene blue dye from aqueous solution*. *J. Appl. Biotechnol. Bioeng.* 5 (2018).
6. Li, B., Guo, J., Lv, K. & Fan, J. *Adsorption of methylene blue and Cd(II) onto maleylated modified hydrochar from water*. *Environ. Pollut.* 254 (2019) 113014.
7. Khan, I. *et al. and Photodegradation*. (2022).
8. Sahu, S. *et al. Adsorption of methylene blue on chemically modified lychee seed biochar: Dynamic, equilibrium, and thermodynamic study*. *J. Mol. Liq.* 315 (2020) 113743.
9. LabChem. *Methylene Blue Safety Data Sheet*. *LabChem Perform. though Chem.* 7 (2012) 1–7.
10. Li, B. *et al. The polyaminocarboxylated modified hydrochar for efficient capturing methylene blue and Cu(II) from water*. *Bioresour. Technol.* 275. (2019) 360–367.
11. Kambo, H. S. & Dutta, A. *A comparative review of biochar and hydrochar in terms of production, physico-chemical properties and applications*. *Renew. Sustain. Energy Rev.* 45 (2015) 359–378.
12. Maniscalco, M. P., Volpe, M. & Messineo, A. *Hydrothermal carbonization as a valuable tool for energy and environmental applications: A review*. *Energies* 13 (2020).
13. Jain, A., Balasubramanian, R. & Srinivasan, M. P. *Hydrothermal conversion of biomass waste to activated carbon with high porosity: A review*. *Chem. Eng. J.* 283 (2016) 789–805.
14. Sevilla, M. & Fuertes, A. B. *The production of carbon materials by hydrothermal carbonization of cellulose*. *Carbon N. Y.* 47 (2009) 2281–

2289.
15. Qian, W. C., Luo, X. P., Wang, X., Guo, M. & Li, B. *Removal of methylene blue from aqueous solution by modified bamboo hydrochar*. *Ecotoxicol. Environ. Saf.* 157 (2018) 300–306.
16. Madduri, S., Elsayed, I. & Hassan, E. B. *Novel oxone treated hydrochar for the removal of Pb(II) and methylene blue (MB) dye from aqueous solutions*. *Chemosphere* 260 (2020) 127683.
17. Tu, W. *et al*. *A novel activation-hydrochar via hydrothermal carbonization and KOH activation of sewage sludge and coconut shell for biomass wastes: Preparation, characterization and adsorption properties*. *J. Colloid Interface Sci.* 593 (2021) 390–407.
18. Tran, T. H. *et al. Comparative study on methylene blue adsorption behavior of coffee husk-derived activated carbon materials prepared using hydrothermal and soaking methods*. *J. Environ. Chem. Eng.* 9 (2021) 105362.
19. Statistik, B. P. *Statistik Tebu Indonesia 2019*. *Badan Pus. Stat.* (2019) 23.
20. Lestari, D. I. *Adsorpsi Methylene Blue Menggunakan Hydrochar Teraktivasi dari Ampas Tebu: Studi Kinetika, Isotherm dan Termodinamika*. (Universitas Gadjah Mada, 2021).
21. Kumar, P. & Chauhan, M. S. *Adsorption of chromium (VI) from the synthetic aqueous solution using chemically modified dried water hyacinth roots*. *J. Environ. Chem. Eng.* 7 (2019) 103218.
22. Mpatani, F. M. *et al*. *Removal of methylene blue from aqueous medium by citrate modified bagasse: Kinetic, Equilibrium and Thermodynamic study*. *Bioresour. Technol. Reports* 11 (2020) 100463.
23. Ho, Y. S. & McKay, G. *Pseudo-second order model for sorption processes*. *Process Biochem.* 34 (1999) 451–465.
24. Wang, J. & Guo, X. *Adsorption kinetic models: Physical meanings, applications, and solving methods*. *J. Hazard. Mater.* 390 (2020) 122156.
25. Parra-Marfíl, A. *et al. Synthesis and characterization of hydrochar from industrial Capsicum annuum seeds and its application for the adsorptive removal of methylene blue from water*. *Environ. Res.* 184 (2020) 109334.
26. Mäkelä, M., Volpe, M., Volpe, R., Fiori, L. & Dahl, O. *Spatially resolved spectral determination of polysaccharides in hydrothermally carbonized biomass*. *Green Chem.* 20 (2018) 1114–1120.
27. Ogihara, Y., Smith, R. L., Inomata, H. & Arai, K. *Direct observation of cellulose dissolution in subcritical and supercritical water over a wide range of water densities (550-1000 kg/m3)*. *Cellulose* 12 (2005) 595–606.
28. Ahmad, T. Y., Hirajima, T., Kumagai, S. & Sasaki, K. *Production of solid biofuel from agricultural wastes of the palm oil industry by hydrothermal treatment*. *Waste and Biomass Valorization* 1 (2010) 395–405.
29. dos Santos, J. V. *et al. Hydrothermal carbonization of sugarcane industry by-products and process water reuse: structural, morphological, and fuel properties of hydrochars*. *Biomass Convers. Biorefinery* (2021).
30. Kruse, A., Funke, A. & Titirici, M. M. *Hydrothermal conversion of biomass to fuels and energetic materials*. *Curr. Opin. Chem. Biol.* 17 (2013) 515–521.
31. Nandiyanto, A. B. D., Oktiani, R. & Ragadhita, R. *How to read and interpret ftir spectroscope of organic material*. *Indones. J. Sci. Technol.* 4 (2019) 97–118.
32. Al-Ghouti, M. A. & Al-Absi, R. S. *Mechanistic understanding of the adsorption and thermodynamic aspects of cationic methylene blue dye onto cellulosic olive stones biomass from wastewater*. *Sci. Rep.* 10 (2020) 1–18.
33. Abidin, N. H. Z., Sambudi, N. S. & Kamal, N. A. *Composite of hydroxyapatite-fe3o4 for the adsorption of methylene blue*. *ASEAN J. Chem. Eng.* 20 (2020) 140–153.
34. Jais, F. M., Chee, C. Y., Ismail, Z. & Ibrahim, S. *Experimental design via NaOH activation process and statistical analysis for activated sugarcane bagasse hydrochar for removal of dye and antibiotic*. *J. Environ. Chem. Eng.* 9 (2021) 104829.
35. Kara, A. & Demirbel, E. *Kinetic, isotherm and thermodynamic analysis on adsorption of Cr(VI) ions from aqueous solutions by synthesis and characterization of magnetic-poly (divinylbenzene-vinylimidazole) microbeads*. *Water. Air. Soil Pollut.* 223 (2012) 2387–2403.
36. Bayu, A. *et al. Isotherm adsorption characteristics of carbon microparticles prepared from pineapple peel waste*. *Commun. Sci. Technol.* 5 (2020) 31–39.
37. Li, H.-Z. *et al. Preparation of hydrochar with high adsorption performance for methylene blue by co-hydrothermal carbonization of polyvinyl chloride and bamboo*. *Bioresour. Technol.* 337 (2021) 125442.
38. Zulfajri, M., Kao, Y. T. & Huang, G. G. *Retrieve of residual waste of carbon dots derived from straw mushroom as a hydrochar for the removal of organic dyes from aqueous solutions*. *Sustain. Chem. Pharm.* 22 (2021) 100469.
39. Sun, K., Tang, J., Gong, Y. & Zhang, H. *Characterization of potassium hydroxide (KOH) modified hydrochars from different feedstocks for enhanced removal of heavy metals from water*. *Environ. Sci. Pollut. Res.* 22 (2015) 16640–16651.
40. Tabassum, M. *et al. NaOH-Activated Betel Nut Husk Hydrochar for Efficient Adsorption of Methylene Blue Dye*. *Water. Air. Soil Pollut.* 231 (2020).
41. Lim, Y. S. & Kim, J. H. *Isotherm, kinetic and thermodynamic studies on the adsorption of 13-dehydroxybaccatin III from Taxus chinensis onto Sylopute*. *J. Chem. Thermodyn.* 115 (2017) 261–268.
42. Chen, S. *et al*. *Study on the adsorption of dyestuffs with different properties by sludge-rice husk biochar: Adsorption capacity, isotherm, kinetic, thermodynamics and mechanism*. *J. Mol. Liq.* 285 (2019) 62–74.
43. Yao, Y., Xu, F., Chen, M., Xu, Z. & Zhu, Z. *Adsorption behavior of methylene blue on carbon nanotubes*. *Bioresour. Technol.* 101 (2010) 3040–3046.
44. Mohadi, R. *et al. Removal of Cr(VI) from aqueous solution by biochar derived from rice husk*. *Commun. Sci. Technol.* 6 (2021) 11–17.